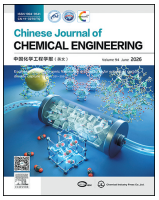
Chinese Journal of Chemical Engineering 94 (2026) 102–112

Contents lists available at ScienceDirect

Chinese Journal of Chemical Engineering

journal homepage: www.elsevier.com/locate/CJChE



Full Length Article

Folate and lipoic acid functionalized pH/reductive dual-responsive mixed crosslinked micelles for paclitaxel delivery



Minghong Feng [1], Teng He [1], Haiqian Zhao [1], Tao Chen [1], Wenjing Lin [1, 2, *], Chufen Yang [1, 2, *]

[1] School of Chemical Engineering and Light Industry, Guangdong University of Technology, Guangzhou 510006, China
[2] Guangdong Provincial Laboratory of Chemistry and Fine Chemical Engineering Jieyang Center, Jieyang 515200, China

ARTICLE INFO

Article history:
Received 14 June 2025
Received in revised form
5 January 2026
Accepted 14 January 2026
Available online 10 March 2026

Keywords:
pH-responsive
Active targeting
Drug-loaded micelles
Crosslinking
Mixed micelles

ABSTRACT

To address the challenges of poor stability and weak targeting capability in polymeric micelles, which negatively impact controlled drug release performance, pH-responsive polymers PCL-PDEAEMA-PHEMA-PPEGMA (P1, P2, and P3) with distinct block lengths were designed and synthesized in this work. These copolymers were rigorously characterized using ^{1}H NMR, FT-IR, and GPC. Subsequently, polymer P3 was selected for modification based on comparative analyses of critical micelle concentrations (CMC) and drug-loading performance. Polymer P3 underwent esterification with lipoic acid (LA) and folic acid (FA) to yield LA-P3 and FA-P3, respectively. These derivatives were blended at a mass ratio of 1:1 (LA-P3:FA-P3), and dithiothreitol was employed to initiate self-crosslinking, resulting in the preparation of actively targeted crosslinked mixed micelles (C-MIX). The results revealed that C-MIX@PTX drug-loaded micelles prepared at a feeding ratio of 15 mg PTX/30 mg polymer exhibited a smaller size (134.7 nm) compared to non-crosslinked micelles, with a drug-loading content of 15.31% ± 1.79% and an encapsulation efficiency of 38.42% ± 5.22%. *In vitro* release studies demonstrated that under neutral conditions, C-MIX@PTX achieved a cumulative drug release of 16.8% at 120 h, significantly lower than non-crosslinked micelles. Under acidic/reductive conditions, C-MIX@PTX showed a cumulative drug release of 77.1% at 120 h, slightly lower compared to non-crosslinked micelles. Cytotoxicity assays confirmed that both MIX and C-MIX were biocompatible low-toxicity carrier materials, while LA-P3@PTX, FA-P3@PTX, MIX@PTX, and C-MIX@PTX exhibited inhibitory effects on HepG2 cells, FA-P3@PTX with folate-modified demonstrated enhanced efficacy.
© 2026 The Chemical Industry and Engineering Society of China, and Chemical Industry Press Co., Ltd. All rights are reserved, including those for text and data mining, AI training, and similar technologies.

1. Introduction

Stimuli-responsive nano-polymeric drug-loaded micelles, capable of flexibly delivering antitumor drugs to overcome physiological and pathological barriers while achieving sustained targeted delivery and controlled release, have emerged as a key research focus in advanced drug delivery systems for reducing drug toxicity and enhancing therapeutic efficacy [1–3]. These nanocarriers are constructed through the self-assembly of amphiphilic polymers in aqueous solution, forming core/shell-structured nanoparticles. The hydrophobic core serves to encapsulate hydrophobic therapeutic agents, significantly improving drug solubility, while the hydrophilic shell stabilizes the micellar structure and provides biological protection. This architecture effectively minimizes drug-induced toxicity in healthy tissues by preventing premature drug release and avoiding recognition by the reticuloendothelial system, thereby reducing hepatic/splenic clearance and renal excretion [4–6].

Functional modification of polymeric micelles through the incorporation of stimuli-responsive moieties or targeting ligands enables intelligent drug delivery by leveraging microenvironmental discrepancies between normal tissues (pH ~7.4, 36–37 °C, low GSH) and tumor tissues (pH 5.0–6.5, 37–42 °C, elevated GSH, and overexpression of proteins/enzymes/receptors). This strategy confers stimuli-responsive behavior and active targeting capabilities, facilitating precision-controlled drug release and enhanced tumor-specific accumulation of chemotherapeutic agents [7–9]. For instance, Pu *et al.* [10] developed pH-responsive amphiphilic poly (ethylene glycol)-imino-poly (benzyl-L-aspartate) (PIPA)

* Corresponding authors.
E-mail addresses: Wenjing.Lin@gdut.edu.cn (W. Lin), cfyang@gdut.edu.cn (C. Yang).

https://doi.org/10.1016/j.cjche.2026.01.013
1004-9541/© 2026 The Chemical Industry and Engineering Society of China, and Chemical Industry Press Co., Ltd. All rights are reserved, including those for text and data mining, AI training, and similar technologies.

micelles for hydroxycamptothecin (HCPT) delivery. The system demonstrated sustained drug retention at physiological pH 7.4 (<15% release in 24 h) while exhibiting accelerated drug release (82% cumulative release) under tumor-acidic conditions (pH 5.0) due to protonation-induced micellar destabilization. Similarly, Luo *et al.* engineered redox-responsive mPEG-*b*-PMA-SS-VE (PSSV) micelles covalently conjugated with cisplatin *via* disulfide linkages [11]. Under high GSH concentrations, reductive cleavage of disulfide bonds triggered micellar disassembly and rapid drug release (3.5-fold faster than physiological GSH levels). Wang *et al.* [12] employed click chemistry to graft folate (FA) ligands onto PCL-SS-POEGMA copolymers, creating FA-functionalized micelles for doxorubicin (DOX) delivery. Comparative *in vitro*/*in vivo* studies revealed superior tumor targeting (1.8-fold higher cellular uptake in FRα-overexpressing cells) and antitumor efficacy (73.2% tumor inhibition rate *vs.* 51.4% for non-targeted micelles) in FA-modified systems, as validated by fluorescence imaging and pharmacodynamic evaluations.

Despite significant advances in stimuli-responsive polymeric drug-loaded micelles as novel delivery systems for anticancer agents, critical challenges persist in optimizing their comprehensive performance, particularly regarding drug loading capacity, controlled release precision, and targeting efficiency [13–16]. Based on our group's previous studies, we have demonstrated that mixed micelle systems constructed through the strategic combination of two or more distinct polymers exhibiting superior functional integration compared to single-polymer micelles. This approach enabled synergistic incorporation of multifunctional blocks, resulting in enhanced critical micelle concentration (CMC) values, drug loading efficiency (up to 28.5%), controlled release, and active targeting capabilities [17–20]. Our group then developed a mixed micellar system comprising PPEGMA-PDEAEMA and PCL-PPEGMA copolymers for DOX delivery. Systematic optimization of the PPEGMA-PDEAEMA/PCL-PPEGMA mass ratio (1:2 to 2:1) yielded pH-responsive nanocarriers with high drug loading (22.3% ± 1.7%) and negligible initial burst release (<3% at pH 7.4 over 8 h) [21]. Furthermore, we developed a folate-functionalized pH/reduction dual-responsive mixed micelles system (DOX@FA-PEG-PDEAEMA/PEG-SS-PCL). This system combined pH-sensitive PDEAEMA segments (pK_a ~6.9) with reduction-labile SS bonds, achieving GSH-triggered drug release and FA-mediated targeting. Comparative studies revealed 41.7% greater tumor growth inhibition versus non-targeted counterparts [22]. However, these mixed systems still faced limitations in structural stability during systemic circulation, with observed premature drug leakage and partial micelle disassembly under complicated conditions.

To resolve these limitations, crosslinked micelles with reversible chemical bonds between polymer chains or drug molecules have been extensively validated as an effective approach to prevent micelle dissociation and enhance structural stability [23–26]. Notably, Kuang *et al.* [27] developed a redox-sensitive disulfide-based core-crosslinked polymeric micelle system (mPEG-*b*-PLL/LA) for DOX encapsulation. After dithiothreitol (DDT)-initiated LA autocrosslinking, the resulting crosslinked drug-loaded micelles (CLM@DOX) demonstrated enhanced stability under physiological conditions, effectively minimizing premature drug release (<8% cumulative release in PBS pH 7.4 over 48 h). Crucially, the disulfide crosslinkers exhibited selective cleavage in response to elevated intracellular GSH concentrations (10 $mmol \cdot L^{-1}$), triggering micellar disassembly and controlled drug release (82.3% ± 3.1% at 24 h under tumor-mimetic conditions). Thus, although studies on micelles combining folic acid targeting and disulfide bond crosslinking have been reported, their synthesis tends to be relatively complex, and achieving synergy between multiple functions remains challenging. Current mixed cross-linked micelle systems, on the other hand, often provide only individual features, such as folate targeting alone, cross-linking alone, or single responsiveness. However, mixed-crosslinked micelles that simultaneously address the issues of high stability, high drug loading capacity, excellent multi-responsive controlled release performance, and targeted delivery remain rarely reported.

To address above problems in previously works, our current study proposed a three-in-one strategy that employed a crosslinking approach to design and synthesize folic acid/lipoic acid (FA/LA)-functionalized pH/reduction dual-responsive mixed crosslinked micelles for the delivery of the anticancer drug paclitaxel (PTX). The structural configuration, preparation process, and drug release mechanism of the mixed crosslinked PTX-loaded micelles were shown in Fig. 1. The pH-responsive polymer PCL-PDEAEMA-PHEMA-PPEGMA was synthesized *via* ring-opening polymerization (ROP) of ε-caprolactone (ε-CL) and atom transfer radical polymerization (ATRP) of 2-(diethylamino) ethyl methacrylate (DEAEMA), 2-hydroxyethyl methacrylate (HEMA), and poly (ethylene glycol) methyl ether methacrylate (PEGMA). The synthesized polymer was subsequently esterified with lipoic acid (LA) or folic acid (FA) to obtain LA-modified polymer (LA-P) or FA-conjugated polymer (FA-P), respectively. LA-P and FA-P were co-assembled into mixed micelles (MIX) through solvent evaporation, followed by DTT-induced self-crosslinking of LA moieties within the micellar core to yield mixed crosslinked micelles (C-MIX). The DEAEMA block conferred pH-responsive behavior to the micelles, maintaining the stability of the hydrophobic core under normal physiological pH while undergoing protonation in the acidic tumor microenvironment, leading to structural loosening and initial facilitation of drug release. The incorporated lipoic acid (LA) further enhanced the physiological stability of the micelles *via* self-crosslinking, while its disulfide bonds underwent specific cleavage in the highly reductive intracellular environment of tumor cells. This reduction response acted synergistically with the pH-triggered structural change to enable efficient drug release. Moreover, folate (FA) modification not only conferred active tumor-targeting capability to the carrier but also contributes to stabilizing the core–shell structure of the micelles through cooperative assembly. This integrated design combined structural stability, targeted delivery, and dual-responsive controlled release, providing a robust platform for constructing highly efficient and low-toxicity drug delivery systems.

2. Materials and Methods

2.1. Experimental materials

ε-CL (99%, Macklin), *n*-butanol (98%, Macklin), copper(II) bromide ($CuBr_2$, 99%, Macklin), *n*-hexane (AR, Sinopharm), tin(II) 2-ethylhexanoate ($Sn(Oct)_2$, 95%, Aladdin), DEAEMA (99%, Aladdin), PEGMA (475 Da, Aladdin), HEMA (99%, Aladdin), 2-bromoisobutyryl bromide (BIBB, 98%, Aladdin), N,N,N′,N″,N″-pentamethyldiethylenetriamine (PMDETA, 99%, Aladdin), triethylamine (TEA, AR, Aladdin), tetrahydrofuran (THF, AR, Tianjin Zhiyuan Reagent), potassium bromide (KBr, spectroscopic grade, Aladdin), neutral alumina (200–300 mesh (85–127 nm), Sinopharm), anhydrous magnesium·sulfate (AR, Aladdin), polystyrene (PS, analytical standard, Aladdin), chloroform ($CDCl_3$), pyrene (99%, Aladdin), dimethyl sulfoxide (DMSO, AR, Tianjin Zhiyuan Reagent), acetone (AR, Tianjin Zhiyuan Reagent), paclitaxel (PTX, 99%, Aladdin), phosphate buffer solution (PBS, AR, Energy Chemical), acetate buffer (AR, Tianjin Zhiyuan Reagent), acetate buffer (AR, Tianjin Zhiyuan Reagent), *N*,*N*′-carbonyldiimidazole (CDI, 99%, Aladdin), folic acid (FA, AR), lipoic acid (LA, AR, Tianjin Zhiyuan Reagent), DL-dithiothreitol (DTT, 99%, Aladdin), hepatocellular

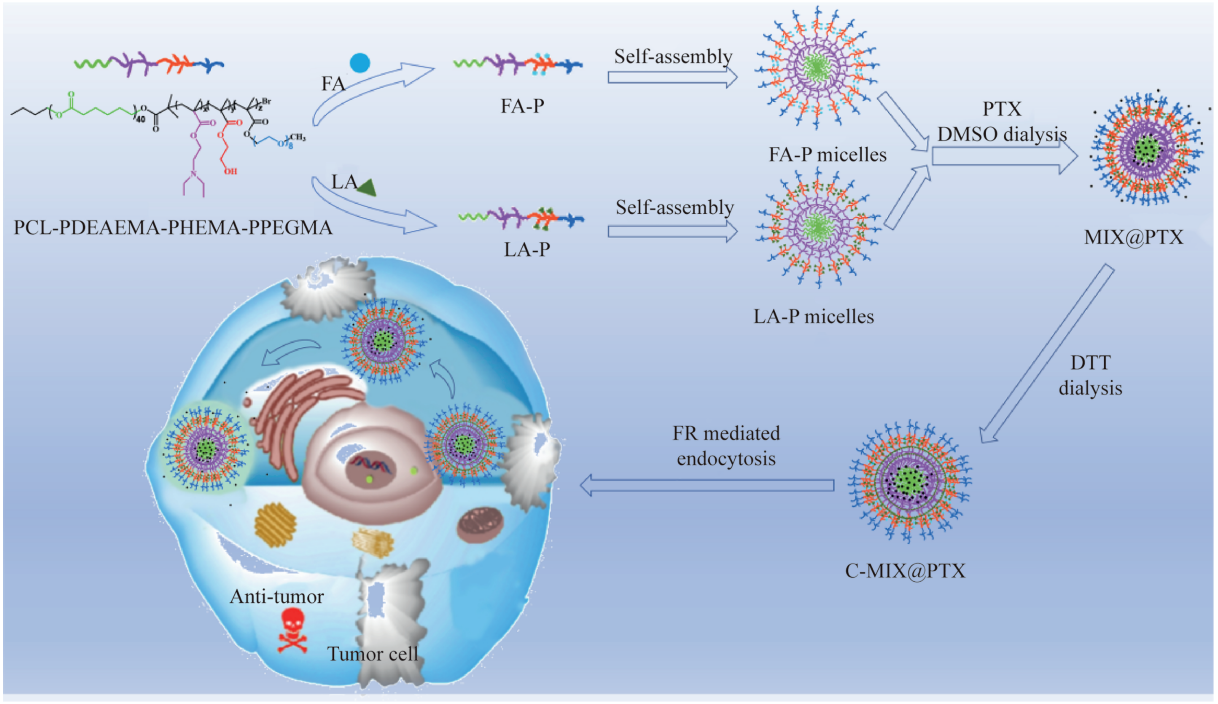


Fig. 1. Structure, preparation and PTX release process of FA -induced pH/reduction dual-response polymer mixed crosslinked PTX-loaded micelles.

carcinoma cells (HepG2 cells, ATCC), DMEM medium (medical grade, Invitrogen). Prior to experiments, 2-(diethylamino)ethyl methacrylate (DEAEMA), 2-hydroxyethyl methacrylate (HEMA), and poly(ethylene glycol) methacrylate (PEGMA) were filtered through a neutral alumina column to remove polymerization inhibitors. The purified monomers were used immediately after purification to prevent spontaneous polymerization.

2.2. Synthesis of the macroinitiator (PCL-Br)

The synthesis of PCL was achieved through ROP catalyzed by $Sn(Oct)_2$, with *n*-butanol serving as the initiator. In a typical procedure, ε-CL (9.13 g, 80.0 mmol), *n*-butanol (0.183 ml, 2.0 mmol), and $Sn(Oct)_2$ (0.027 g, 0.02 mmol) were charged into an 100 ml reaction vessel. Polymerization proceeded at 130 °C for 24 h under continuous nitrogen purging. The resultant mixture was cooled to ambient temperature, dissolved in THF, and concentrated by rotary evaporation. Purification was accomplished by precipitation in chilled *n*-hexane, yielding PCL as a white powder. This PCL product was subsequently functionalized to generate the macroinitiator PCL-Br *via* bromination. Specifically, PCL (4.56 g, 1.0 mmol) was dissolved in anhydrous THF under nitrogen atmosphere. TEA (1.11 ml, 8 mmol) and BIBB (0.98 ml, 8 mmol) were then introduced dropwise at 0 °C using an ice-water bath. After initial reaction for 2 h at this temperature, the system was warmed to room temperature and stirred for an additional 18 h. The crude product was diluted with THF, filtered through a neutral alumina column to remove salts, and concentrated under reduced pressure. Final isolation was performed by precipitation in ice-cold *n*-hexane, affording PCL-Br as a powdery white solid.

2.3. Synthesis of the polymer PCL-PDEAEMA-PHEMA-PPEGMA

Into a dried 100 ml reaction flask equipped with a stir bar were sequentially added PCL-Br (1.84 g, 0.4 mmol) and $CuBr_2$ (0.0089 g, 0.04 mmol). The flask was sealed and subjected to three vacuum-nitrogen cycles. After purging, 25 ml of anhydrous THF was added, and the mixture was stirred for 10 min to ensure complete dissolution. Subsequently, DEAEMA (0.74 g, 4.0 mmol) and the ligand PMDETA (0.069 g, 0.84 mmol) were added sequentially and stirred for 20 min to form the catalytic complex. Then, a solution of $Sn(Oct)_2$ (0.162 g, 0.84 mmol) in 3 ml of anhydrous THF was introduced, and the mixture was stirred for an additional 20 min before being transferred to an oil bath preheated to 60 °C. After 6 h of reaction, HEMA (0.78 g, 4.0 mmol) was added, followed by PEGMA ($M_n = 475\ g \cdot mol^{-1}$, 2.85 g, 6.0 mmol) after another 6 h. The polymerization was allowed to proceed for an additional 18 h. Upon completion, the reaction was exposed to air and diluted with excess THF. The catalyst was removed by filtration through a neutral alumina column, and the solution was concentrated *via* rotary evaporation. The product was precipitated by dropwise addition into ice-cold *n*-hexane, collected by filtration, and dried under vacuum to afford PCL_{40}-$PDEAEMA_7$-$PHEMA_{13}$-$PPEGMA_{14}$ (P1) as a white solid. By adjusting the feed ratio of DEAEMA, two additional copolymers, PCL_{40}-$PDEAEMA_{11}$-$PHEMA_{15}$-$PPEGMA_{14}$ (P2) and PCL_{40}-$PDEAEMA_{19}$-$PHEMA_{13}$-$PPEGMA_{17}$ (P3), were synthesized under identical conditions.

2.4. Synthesis of LA/FA-modified polymer PCL-PDEAEMA-P(HEMA-g-LA/FA)-PPEGMA

A magnetic stir bar and LA (0.75 mmol, 0.155 g) were introduced into an oven-dried 100 ml reaction flask. The flask was subsequently sealed and subjected to three consecutive vacuum-argon cycles to establish an inert atmosphere. Following the addition of 20 ml DMSO, the mixture underwent sonication to achieve complete dissolution. CDI (0.75 mmol, 0.122 g) was then added to the solution, which was magnetically stirred at ambient temperature until a homogeneous mixture formed. This mixture was maintained at room temperature for 5 h to facilitate carboxyl group activation. Subsequently, a pre-dissolved solution of polymer P3 (0.05 mmol, 0.87 g in anhydrous DMSO) was introduced

into the reaction vessel. The reaction was allowed to proceed at room temperature for an additional 18 h. Upon reaction completion, the resulting solution was transferred into a dialysis membrane (MWCO 3500) and dialyzed exhaustively against deionized water for 48 h, with the dialysate being replaced at 4-h intervals. The dialyzed solution was subsequently filtered through a 0.45 μm microporous membrane and lyophilized, yielding the LA-functionalized polymer designated as PCL-PDEAEMA-P(HEMA-*g*-LA)-PPEGMA (LA-P3). Utilizing an equimolar quantity of FA (0.331 g) replaced LA, the analogous FA-modified polymer PCL-PDEAEMA-P(HEMA-*g*-FA)-PPEGMA (FA-P3) was synthesized under identical reaction conditions.

2.5. Structural characterization of the polymers

The synthesized polymers PCL-PDEAEMA-PHEMA-PPEGMA and their intermediates were characterized by ^{1}H nuclear magnetic resonance (^{1}H NMR) spectroscopy on a Bruker AVANCE III 400 MHz spectrometer using tetramethylsilane (TMS) as the internal standard and deuterated chloroform ($CDCl_3$) or deuterated dimethyl sulfoxide (DMSO-d_6) as the solvent. The measurement was performed at a frequency of 400 Hz and room temperature. Fourier transform infrared (FT-IR) spectra of the polymers were recorded on a Nicolet 6700 spectrometer (Thermo Fisher Scientific, USA) using spectroscopic grade potassium bromide (KBr) pellets. The spectra were collected in the range of 4000–500 cm^{-1} at room temperature. The M_n and polydispersity index (M_w/M_n) of PCL, PCL-Br, P_3, FA-P3 and LA-P3 were determined by gel permeation chromatography (GPC) using an Agilent 1200 system with THF as the mobile phase at a flow rate of 1.0 ml·min^{-1}. The measurements were conducted at ambient temperature using appropriate standards.

2.6. Determination of critical micelle concentration

The critical micelle concentration (CMC) of polymers P1, P2, and P3 was determined using pyrene as a fluorescent probe with a Hitachi F-4500 fluorescence spectrophotometer [28]. A 0.1 ml aliquot of 1×10^{-5} mol·L^{-1} pyrene/acetone solution was added to multiple volumetric flasks. After acetone evaporation, aqueous solutions of copolymer micelles with varying concentrations (0.0001–0.1 mg·ml^{-1}) were added to achieve a final pyrene concentration of 6×10^{-7} mol·L^{-1}. The solutions were equilibrated in the dark for 24 h prior to measurement. The CMC value was identified as the inflection point in the plot of the intensity ratio (I_{337}/I_{332}) of pyrene excitation spectra at 337 nm and 332 nm *versus* the logarithm of polymer concentration.

2.7. Preparation and characterization of micelles

Both blank and PTX-encapsulated micellar systems were fabricated *via* the dialysis technique. In a standardized procedure, 30 mg of polymer P1 was dissolved in 30 ml of DMSO through 20-min sonication, with subsequent introduction of PTX (0, 5, 10, 15, 20 or 30 mg). The mixture underwent continuous agitation for 18 h prior to transferal into a dialysis membrane (MWCO 3500 Da). Dialysis against deionized water was conducted over 48 h, incorporating periodic replenishment of the external aqueous phase at 4 h intervals. Subsequent filtration through a 0.45 μm microporous membrane and lyophilization yielded micellar powders. An identical methodology was employed to prepare micelles derived from polymers P2, P3, LA-P3, and FA-P3. For mixed micelle fabrication, combinatorial dissolution of 15 mg LA-P3 and 15 mg FA-P3 with PTX (0 or 15 mg) in 30 ml DMSO preceded 48 h dialysis. The resultant colloidal dispersion was subjected to membrane filtration (0.45 μm) and cryodesiccation, affording blank mixed micelles (MIX) and PTX-loaded mixed micelles (MIX@PTX). A separate portion of the solution was treated with a trace amount of DTT and then dialyzed for 24 h. Subsequent filtration and freeze-drying yielded the cross-linked mixed blank micelles (C-MIX) and the cross-linked mixed drug-loaded micelles (C-MIX@PTX).

$$\mathrm{LC} = \frac{\text{mass of loaded drug}}{\text{mass of micelle}} \times 100\% \tag{1}$$

$$\mathrm{EE} = \frac{\text{mass of loaded drug}}{\text{mass of drug in feed}} \times 100\% \tag{2}$$

2.8. In vitro drug release

The PTX release behavior of PTX-loaded micelles was evaluated *in vitro* using buffer solutions simulating different physiological environments: pH 5.0/10 mmol·L^{-1} DTT to mimic the tumor microenvironment, and pH 7.4/0 mmol·L^{-1} DTT to simulate normal tissue conditions. For comparative purposes, additional control conditions were established using pH 5.0/0 mmol·L^{-1} DTT and pH 7.4/10 mmol·L^{-1} DTT buffer solutions. The PTX-loaded micelle powder (5 mg) was dissolved in 5 ml of the aforementioned buffer solution and transferred into a dialysis bag (MWCO 3500), which was then immersed in 95 ml of the corresponding buffer solution. The dialysis system was maintained at 37 °C with constant stirring at 100 r·min^{-1}. At predetermined time intervals, 5 ml of the external solution was collected as samples, with simultaneous replenishment of 5 ml fresh corresponding buffer to maintain a constant total volume of 100 ml. The absorbance of each sample at 230 nm was measured to calculate the PTX cumulative release percentage (E_r) in different environments using Eq. (3). All experiments were performed in triplicate.

$$E_r = \frac{V_e \sum_{1}^{n-1} C_i + V_0 C_n}{m_d} \times 100\% \tag{3}$$

where C_i represents the concentration of PTX at the ith sampling, n denotes the total number of samplings, and m_d indicates the mass of PTX in PTX-loaded micelles, $V_e = 5$ ml, $V_0 = 100$ ml.

2.9. Cytotoxicity evaluation

The cytotoxicity of polymers, blank micelles, and PTX-loaded micelles against hepatocellular carcinoma cells (HepG2) was evaluated using the CCK-8 assay [29]. Cell suspensions were seeded in 96-well plates at a density of 1×10^4 cells/well and incubated for 24 h (37 °C, 5% CO_2). Subsequently, various concentrations of free PTX, blank micelles, and PTX-loaded micelles were added to each well, along with blank control and DMSO control groups. After 48 h of incubation in the dark, 10 μl of CCK-8 solution was added to each well. Following an additional 4 h incubation, the absorbance at 450 nm was measured using a microplate reader, and cell viability was calculated according to Eq. (4).

$$\text{Cell viability} = \frac{A_{\text{sample}} - A_{\text{blank}}}{A_{\text{control}} - A_{\text{blank}}} \times 100\% \tag{4}$$

where A_{sample} represents the absorbance of the sample well, A_{blank} denotes the absorbance of the blank well, and $A_{control}$ indicates the absorbance of the control group.

3. Results and Discussion

3.1. Synthesis and characterization of polymers

The synthetic route of PCL-PDEAEMA-PHEMA-PPEGMA (P) was illustrated in Fig. S1, with the ^{1}H NMR characterization results of its intermediates PCL and PCL-Br (−C(CH$_3$)$_2$−Br, 1.93) shown in Fig. S2. PCL was first synthesized *via* ROP of ε-CL using *n*-butanol as the initiator, followed by bromination to yield PCL-Br. Through ARGET ATRP reaction under controlled monomer feed ratios in the presence of catalyst and ligand, PCL-PDEAEMA-PHEMA-PPEGMA with varying degrees of polymerization was obtained, whose FT-IR and ^{1}H NMR spectra were presented in Fig. 2(a) and (d), respectively. The synthetic routes for LA-P3 and FA-P3 were depicted in Fig. S3, with their corresponding FT-IR and ^{1}H NMR characterization results shown in other panels of Fig. 2.

The FT-IR spectra in Fig. 2(a) demonstrated that compared with the PCL spectrum, both PCL-Br and P3 spectra exhibited a stretching vibration peak of the bromine-carbon bond in PCL-Br at 643 cm^{-1}. Moreover, the P3 spectrum displayed a distinct hydroxyl characteristic peak at 3500 cm^{-1} originating from the hydroxyl group of 2-hydroxyethyl methacrylate monomer. The peaks observed at 2932 cm^{-1} and 2848 cm^{-1} corresponded to the methyl and methylene groups in the PCL segment, confirming successful incorporation of PCL blocks into the polymer. Characteristic absorption bands at 1728 cm^{-1} and 1250 cm^{-1} were attributed to the carbonyl group and ether bond of the PDEAEMA block, respectively. Notably, the absence of characteristic peaks for vinyl C=C bonds at 1640 cm^{-1} indicated complete monomer conversion, providing further evidence for the successful synthesis of the target polymer.

The FT-IR spectra in Fig. 2(b) and (c) revealed that the characteristic peaks of PCL, PDEAEMA, and PEGMA blocks from the aforementioned P3 remained present in both LA-P3 and FA-P3. Fig. 2(b) further demonstrated the disappearance of the hydroxyl stretching vibration peak at 3500 cm^{-1} and the carboxyl stretching vibration peak of LA at 1760 cm^{-1}, indicating the occurrence of esterification and successful grafting of LA onto the polymer through its carboxyl group. As shown in Fig. 2(c), the appearance of stretching vibration peaks at 3416 cm^{-1} and 3220 cm^{-1} corresponding to the −NH$_2$ group in FA, along with the aromatic ring stretching vibrations at 1570 cm^{-1} and 1488 cm^{-1}, confirmed the successful grafting of folic acid onto the polymer.

The ^{1}H NMR spectrain Fig. 2(d) revealed characteristic chemical shifts corresponding to distinct polymer blocks: $\delta_r = 4.05$, $\delta_k = 2.$ ppm, $\delta_{p,q} = 1.65$, and $\delta_l = 1.37$ were attributed to the PCL segment. The PDEAEMA block exhibited characteristic shifts at $\delta_d = 2.72$, $\delta_e = 2.59$, $\delta_C = 4.05$, and $\delta_f = 1.06$. Peaks at $\delta_H = 3.64$ and $\delta_g = 3.82$ corresponded to methylene groups in the PHEMA block, while $\delta_i = 4.05$, $\delta_j = 3.64$, and $\delta_m = 3.38$ were assigned to the PPEGMA segment. The peak at $\delta_b = 1.90$ originated from methylene groups formed by double bond cleavage during block coupling, and $\delta_a = 0.84$ represented methyl groups adjacent to inter-block linkages. These characteristic shifts collectively confirmed successful

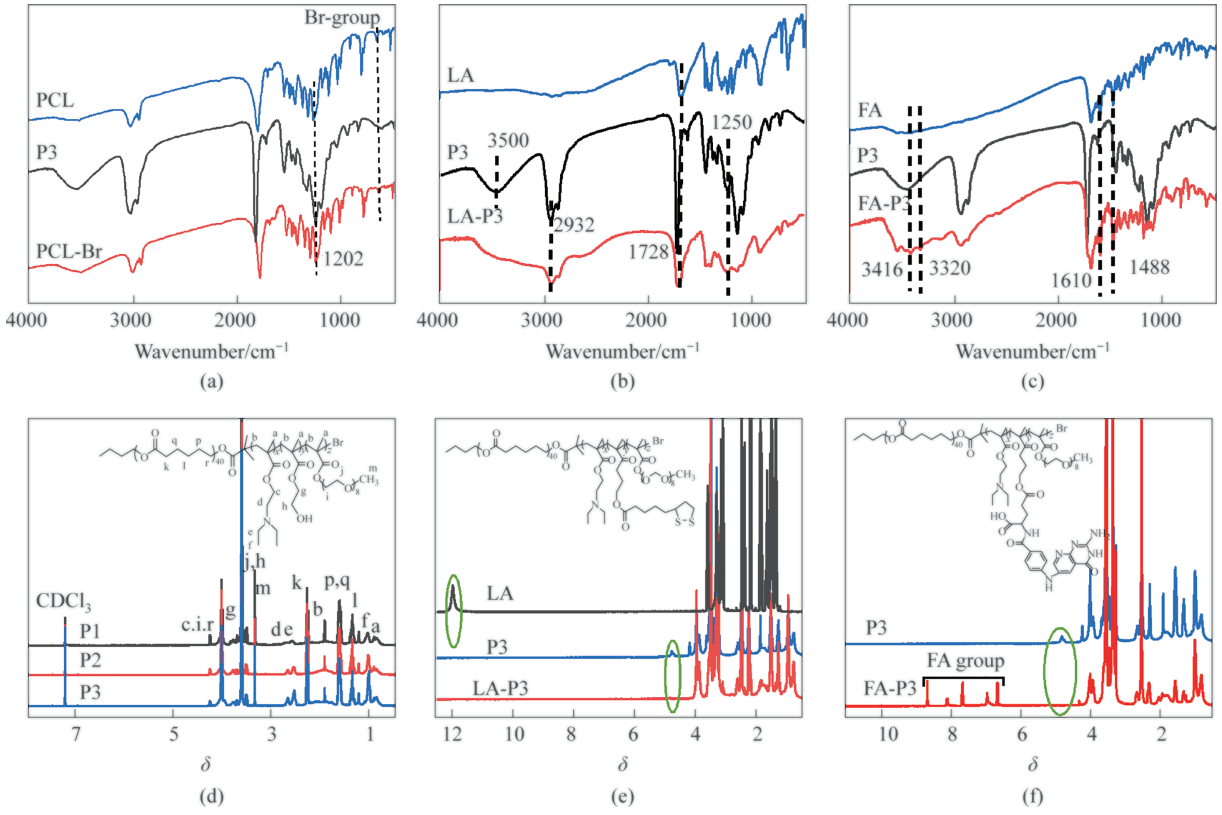


Fig. 2. FT IR of PCL$_{40}$, PCL$_{40}$-Br, PCL$_{40}$-PDEAEMA$_{19}$-PHEMA$_{13}$-PPEGMA$_{17}$ (P3) (a); LA, LA-P3 (b); FA, FA-P3 (c); ^{1}H NMR spectra of P1, P2, P3 (d); LA, LA-P3(e); FA, FA-P3(f).

Table 1
GPC and ^{1}H NMR results of polymers.

Sample①	$M_{n,TH}$②	$M_{n,NMR}$③	$M_{n,GPC}$④	PDI④
PCL_{40}	4634	4634	4410	1.39
PCL_{40}-Br	4783	4783	4537	1.42
PCL_{40}-$PDEAEMA_7$-$PHEMA_{13}$-$PPEGMA_{14}$ (P1)	15708	14418	15416	1.23
PCL_{40}-$PDEAEMA_{11}$-$PHEMA_{15}$-$PPEGMA_{14}$ (P2)	16633	15418	16244	1.20
PCL_{40}-$PDEAEMA_{19}$-$PHEMA_{13}$-$PPEGMA_{17}$ (P3)	17558	18063	17146	1.11
LA-P3	20378	20070	19432	1.37
FA-P3	23903	21809	21265	1.49

① The subscripts of PDEAEMA, PHEMA and PPEGMA were respectively the DP of PDEAEMA (x), PHEMA (y) and PPEGMA (z) calculated from ^{1}H NMR spectra.
② Theoretical molecular weight calculated based on the polymer's molecular formula.
③ Calculated by the equations $M_{n,NMR} = (185x+130y + 475z)\,x + 4799$.
④ Determined by GPC.

integration of all PCL-PDEAEMA-PHEMA-PPEGMA blocks. Furthermore, the proportional increase in peak area ratios at $\delta_d = 2.72$ and $\delta_e = 2.59$ for PDEAEMA segments across three polymers (P1, P2, P3).

Fig. 2(e) showed that the hydroxyl proton signal of the PHEMA block at $\delta = 4.8$ in polymer P3 essentially disappeared after esterification, while characteristic splitting patterns of LA emerged between $\delta = 0.8$ and 3.2. The disappearance of the LA characteristic peak at $\delta = 12$ further supported the successful synthesis of LA-P3. Similarly, in the FA-P3 spectrum, the disappearance of the hydroxyl peak at $\delta = 4.8$ from P3 and the emergence of characteristic FA signals collectively confirmed the successful synthesis of FA-P3 (Fig. 2(f)).

The structural composition of all polymers was characterized by GPC. All GPC curves exhibited monomodal and symmetrical distributions (Fig. S3 and Table 1), indicating well-controlled ROP and ATRP processes with narrow M_w/M_n. The M_w/M_n remained below 1.50, confirming their suitability for subsequent PTX delivery applications. The degree of polymerization (DP) of PDEAEMA (x), PHEMA (y) and PPEGMA (z) per arm as well as the molecular weights ($M_{n,NMR}$) were calculated from the integration ratio values of signals (e) to (p) (I_e/I_p), signals (g to (p) (I_g/I_p) and signals (m) to (p) (I_m/I_p) in Fig. 2(d), respectively. The evidence of ^{1}H NMR spectra summarized in Table 1 was in good agreement with both theoretical predictions and $M_{n,GPC}$ results, suggesting that well-defined copolymers with different block contents had been successfully synthesized and characterized.

Table 2
Size, PDI, LC and EE of PTX-loaded micelles.

Sample	PTX/Polymer /mg·mg^{-1}	Size/nm	PDI	LC/%	EE/%
P1	0/30	75.5 ± 4.1	0.20	-	-
	5/30	78.7 ± 3.9	0.21	10.06 ± 2.28	53.3 ± 4.46
	10/30	82.2 ± 5.1	0.22	12.77 ± 1.94	49.21 ± 3.42
	15/30	90.6 ± 6.8	0.14	15.03 ± 1.38	46.00 ± 5.22
	20/30	92.3 ± 4.2	0.25	15.44 ± 1.66	43.12 ± 4.37
	30/30	111.4 ± 7.1	0.26	16.94 ± 2.82	39.43 ± 3.34
P2	0/30	77.8 ± 4.3	0.25	-	-
	5/30	82.4 ± 4.7	0.17	10.66 ± 1.09	51.64 ± 3.45
	10/30	87.1 ± 7.6	0.18	12.89 ± 3.14	51.22 ± 6.42
	15/30	93.3 ± 3.4	0.26	15.11 ± 1.46	48.00 ± 6.01
	20/30	94.9 ± 6.5	0.19	15.98 ± 2.12	44.21 ± 2.19
	30/30	112.9 ± 9.4	0.27	17.17 ± 1.28	41.55 ± 3.08
P3	0/30	83.1 ± 4.9	0.24	-	-
	5/30	86.5 ± 5.2	0.17	9.84 ± 1.03	57.65 ± 6.63
	10/30	90.0 ± 2.7	0.19	13.96 ± 1.90	53.32 ± 6.14
	15/30	98.4 ± 4.3	0.18	16.23 ± 1.81	51.33 ± 5.76
	20/30	110.3 ± 5.8	0.16	18.24 ± 3.11	47.51 ± 6.93
	30/30	118.8 ± 5.4	0.17	19.33 ± 2.17	43.02 ± 5.96

3.2. Properties of PCL-PDEAEMA-PHEMA-PPEGMA polymeric micelles with different block

The CMCs of different block PCL-PDEAEMA-PHEMA-PPEGMA polymers (P1, P2, and P3) were determined *via* fluorescence spectroscopy, with corresponding values of 4.36, 2.25 and 1.09 mg·L^{-1}, respectively, as illustrated in Fig. 3(a). Notably, polymer P3 exhibited the lowest CMC value. This phenomenon is attributed to the distinct hydrophobic block compositions: P1 possesses the lowest proportion of hydrophobic PCL and PDEAEMA segments, while P3 contains the highest proportion. The inverse correlation between CMC values and hydrophobic block content was well-established, wherein higher hydrophobic segment ratios resulted in lower CMC values. Consequently, the reduced CMC of P3 indicated enhanced stability of its micellar assemblies in aqueous solution.

The particle sizes (determined by DLS) and PTX loading properties of P1, P2, and P3 with varying PTX/polymer feeding ratios were presented in Fig. 3(b) and Table 2. For a given polymer (*e.g.*, P1, P2 or P3), the particle size and LC of the micelles increased with higher PTX feeding ratios, while the EE decreased accordingly. This phenomenon was attributed to the limited solubilization capacity

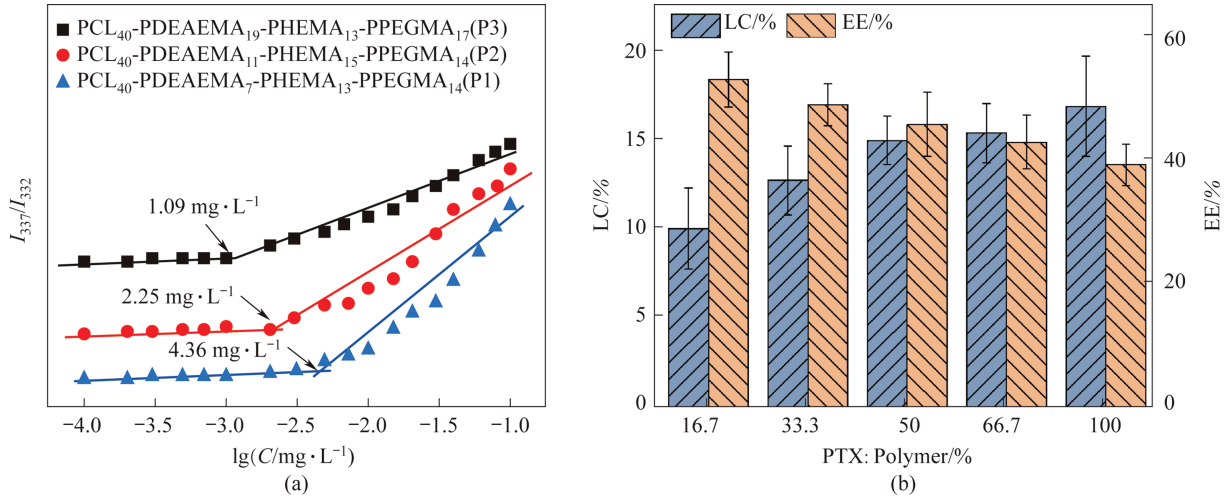


Fig. 3. I_{337}/I_{332} ratios of pyrene in neural aqueous solution of the PCL-PDEAEMA-PHEMA-PPEGMA (a), PTX loading performance of P1 PTX-loaded micelles prepared with different PTX/polymer feeding ratios (b).

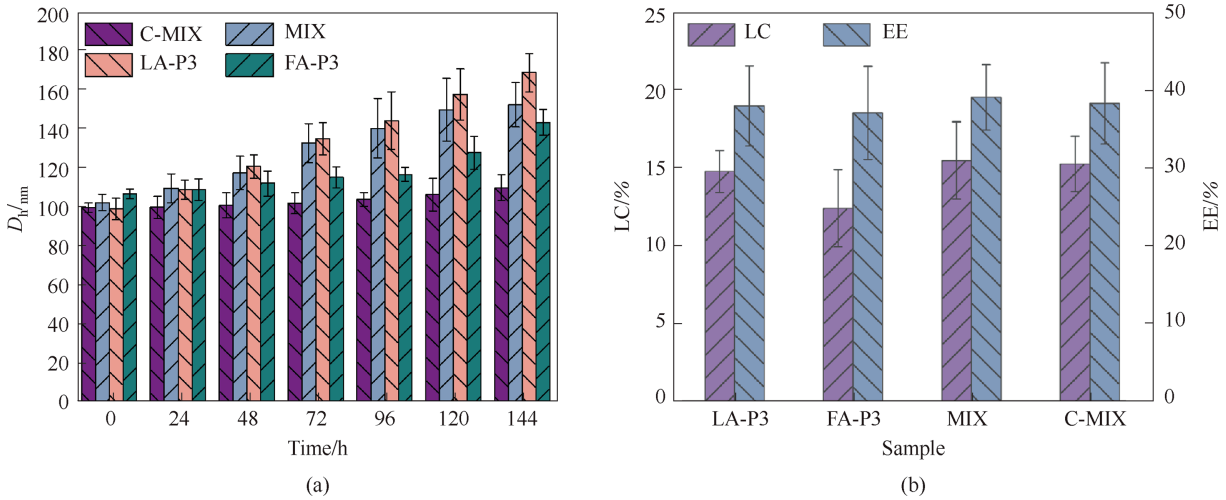


Fig. 4. Stability test results of different micelles in aqueous solution (a), PTX loading performance results of different micelles (b).

Table 3
Size, PDI, LC and EE of PTX-loaded micelles.

Sample	(PTX/Polymer)/mg·mg^{-1}	Size/nm	PDI	LC/%	EE/%
LA-P3	15/30	135.8 ± 1.8	0.14	14.83 ± 1.35	38.09 ± 5.15
FA-P3	15/30	121.3 ± 6.4	0.17	12.46 ± 2.48	37.20 ± 5.99
MIX	15/30	144.9 ± 3.8	0.17	15.54 ± 2.48	39.20 ± 4.21
C-MIX	15/30	134.7 ± 1.9	0.18	15.31 ± 1.79	38.42 ± 5.22

of the hydrophobic core for hydrophobic drugs. Consequently, as the DLC increased, the encapsulation efficiency gradually declined. The optimal PTX/polymer feeding ratio of 15 mg/30 mg achieved both relatively high LC and EE values which therefore was selected for subsequent performance evaluations.

The DLC and EE of PTX-loaded micelles derived from polymers P1, P2, and P3 at a PTX/polymer feeding ratio of 15 mg/30 mg were comparatively analyzed. Notably, micelles fabricated from polymer P3 demonstrated superior LC and EE compared to those of P1 and P2. This enhancement was ascribed to the structural characteristics of the PCL-PDEAEMA-PHEMA-PPEGMA polymer under neutral conditions. Specifically, the hydrophobic blocks of the polymer comprised PCL and PDEAEMA, P3 exhibited a longer PDEAEMA block length than P1 and P2, resulting in an extended total hydrophobic segment. This structural feature enhanced the solubilization capacity for hydrophobic drugs, consequently, P3 achieved the highest LC and EE values of 16.23% ± 1.81% and 51.33% ± 5.76%, respectively. Based on the comprehensive evaluation of CMC values and PTX loading performance among P1, P2, and P3, polymer P3 was selected for subsequent structural modifications and further investigations.

3.3. Performance evaluation of mixed crosslinked micelles

The polymer P3 was individually esterified with LA and FA to obtain LA-P3 and FA-P3, respectively. These derivatives were then mixed at a mass ratio of 1:1 to prepare mixed non-crosslinked micelles (MIX). Subsequently, self-crosslinking of MIX was initiated by DTT to yield mixed crosslinked micelles (C-MIX). The stability of blank micelles (LA-P3, FA-P3, MIX, and C-MIX) in

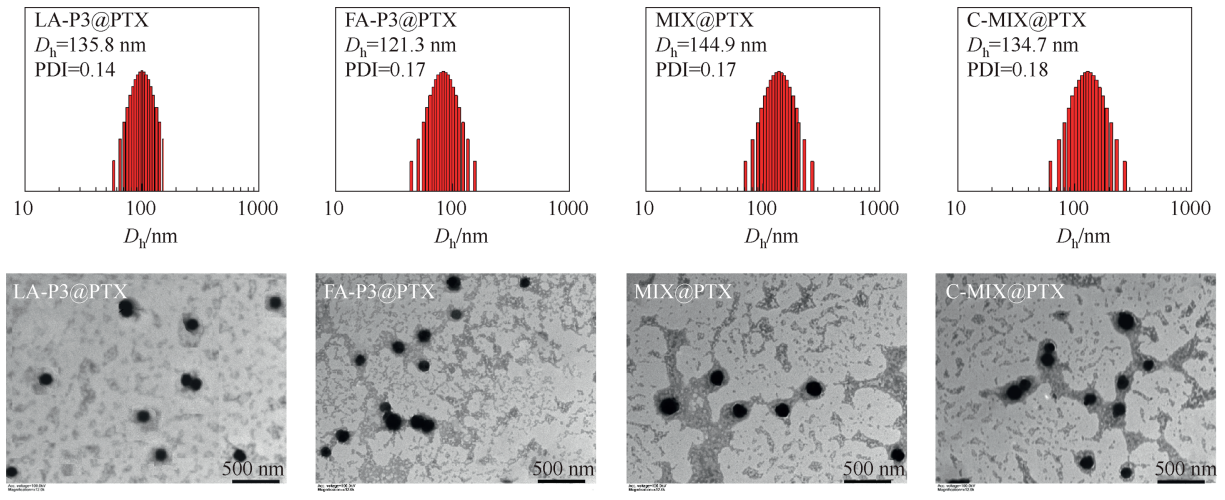


Fig. 5. DLS and TEM images of PTX-loaded micelles.

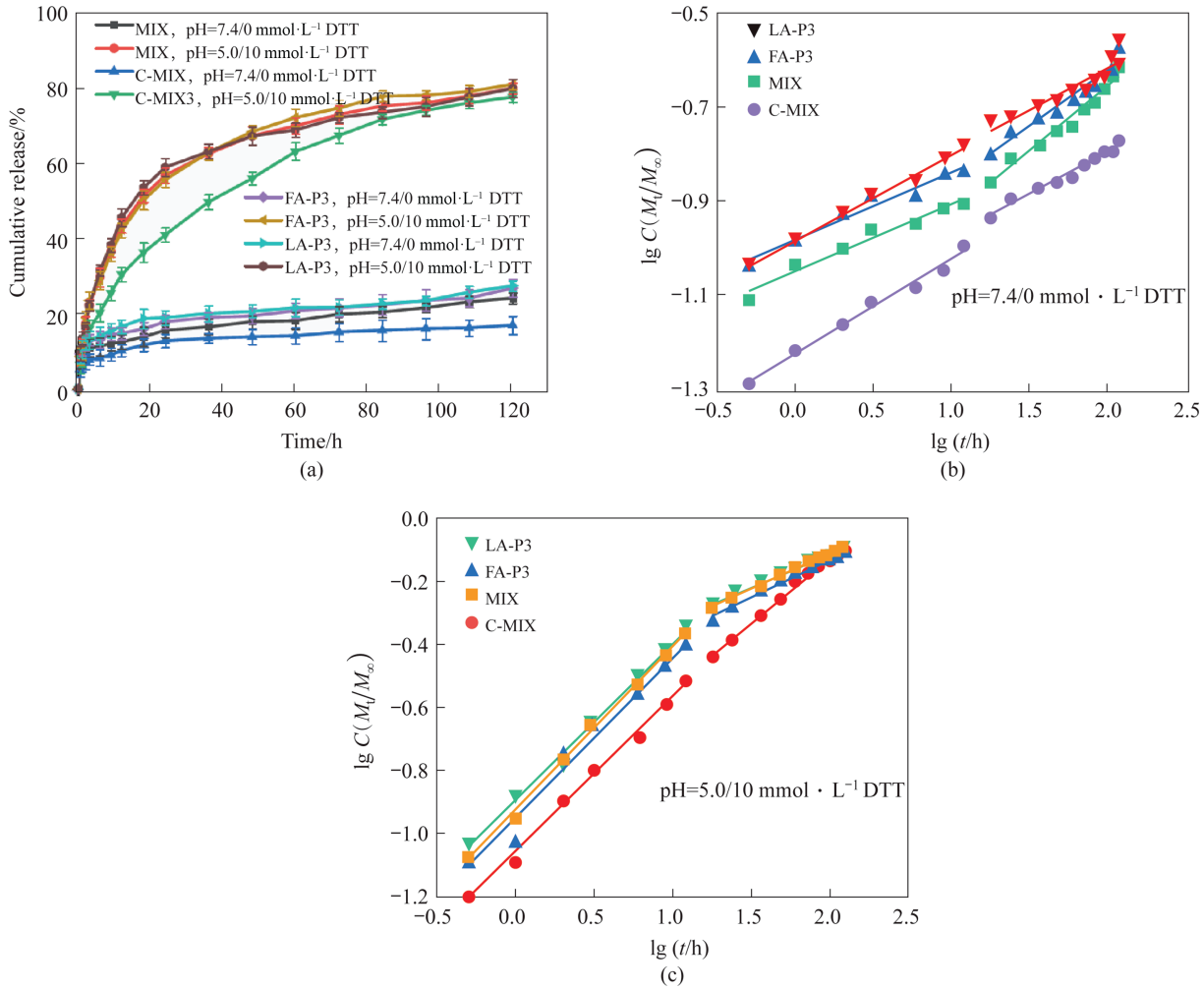


Fig. 6. *In vitro* release curves of PTX-loaded micelles at different pH (a), curve fitting of lg C (M_t/M_∞) to lg t (b)&(c).

aqueous solution was systematically evaluated, as depicted in Fig. 4(a). In a phosphate buffer (pH 7.4), the particle sizes of LA-P3, FA-P3, and MIX micelles progressively increased over time. In contrast, C-MIX exhibited negligible size variation within 144 h, maintaining a consistent diameter range of 100–110 nm. This observation suggested that the crosslinking effect imparted by the LA moieties significantly enhanced micellar stability.

The PTX loading performance of the four micellar systems was summarized in Fig. 4(b) and Table 3. At a PTX/copolymer feeding ratio of 15 mg/30 mg, the PTX-loaded mixed micelles (MIX@PTX) exhibited a LC of 15.54% ± 2.48% and an EE of 39.20% ± 4.21%, marginally higher than those of LA-P3@PTX and FA-P3@PTX. The C-MIX@PTX exhibited a LC of 15.31% ± 1.79% and an EE of 38.42% ± 5.22%, similar to the non-crosslinked MIX@PTX system. TEM images in Fig. 5 revealed that the particle sizes of PTX-loaded micelles (LA-P3@PTX, FA-P3@PTX, MIX@PTX, and C-MIX@PTX) aligned well with the hydrodynamic diameters determined by DLS measurements: were 135.8, 121.3, 144.9 and 134.7 nm, respectively.

The *in vitro* PTX release profiles of four PTX-loaded micellar systems (LA-P3@PTX, FA-P3@PTX, MIX@PTX, and C-MIX@PTX) were shown in Fig. 6(a). As illustrated, LA-P3@PTX, FA-P3@PTX, and MIX@PTX exhibited comparable controlled-release behaviors. Under pH 7.4/0 mmol·L^{-1} DTT conditions, all three systems achieved approximately 25% cumulative PTX release over 120 h, while

Table 4
Fitting parameters of PTX release data at pH 7.4 and 5.0

Sample	pH	$n_1$①	$k_1$①	R_1^2	$n_2$②	$k_2$②	R_2^2
FA-P3	7.4	0.14	0.105	0.956	0.23	0.081	0.974
	5.0	0.51	0.119	0.969	0.25	0.252	0.973
LA-P3	7.4	0.18	0.105	0.994	0.18	0.105	0.849
	5.0	0.50	0.128	0.992	0.20	0.309	0.990
MIX	7.4	0.14	0.090	0.953	0.27	0.063	0.966
	5.0	0.52	0.119	0.995	0.22	0.275	0.987
C-MIX	7.4	0.20	0.060	0.979	0.18	0.071	0.974
	5.0	0.49	0.088	0.993	0.41	0.111	0.990

① The first stage is 0–12 h. ② The second stage is 12–120 h.

under pH 5.0/10 mmol·L^{-1} DTT conditions, their cumulative releases reached ~80% within the same timeframe. This similarity arose from their shared polymer backbone, where LA and FA modifications minimally affected their responsive and stabilizing properties. In contrast, C-MIX@PTX demonstrated enhanced stability in neutral medium (pH 7.4/0 mmol·L^{-1} DTT), with a cumulative release of only 16.8% at 120 h, which represented a substantial reduction in premature PTX leakage compared to non-crosslinked counterparts. Under pH 5.0/10 mmol·L^{-1} DTT conditions, C-MIX@PTX exhibited a slightly lower cumulative release (77.1% at 120 h) than non-crosslinked micelles, accompanied by a

slower initial release rate, suggesting a more sustained release profile attributed to its crosslinked architecture.

Fig. 6(b) and (c) showed the PTX release profiles from micellar carriers, with release mechanisms investigated using the empirical equation proposed by Ritger and Peppas [30].

$$\frac{M_t}{M_\infty} = kt^n \tag{5}$$

$$\lg\left(\frac{M_t}{M_\infty}\right) = n \lg t + \lg k \tag{6}$$

In the equation, M_t and M_∞ represent the cumulative drug release at time "t" and infinite time, respectively; "k" is a constant related to the carrier structure and geometric properties, which correlates with the drug release rate and can be approximated as a rate constant; and "n" is the release exponent, whose value reflects the underlying drug release mechanism. For spherical particles: when $n < 0.43$, release is governed by a combination of diffusion and erosion; when $n = 0.43$, it follows Fickian diffusion; when $0.43 < n < 0.85$, an anomalous transport mechanism prevails, controlled by both diffusion and swelling, indicating random movement of the drug within the swelling matrix; and when $n = 0.85$, a non-Fickian diffusion mechanism operates.

The fitting results indicate that under both pH conditions, the release of PTX from the four micellar systems (MIX, C-MIX, FA-P3, and LA-P3) proceeds through two distinct stages (0–12 h and 12–120 h), with the structure of the crosslinked network being the key factor governing both the release mechanism and the transition in release rates. The corresponding fitting parameters, including n, k, and correlation coefficient (R^2), are summarized in Table 4. As shown in Fig. 6(b) and (c), the fitted lines exhibit good linearity. In the first stage at pH 7.4 with 0 mM DTT, the n values of all four drug-loaded micelles were below 0.43, indicating that PTX release was governed by a combination of diffusion and erosion. Under these conditions, the crosslinked micelle C-MIX@PTX displayed the lowest k value, which was directly attributed to its densely cross-linked core restricting water penetration and polymer chain mobility, thereby significantly reducing the drug diffusion rate and effectively preventing initial burst release. In contrast, at pH 5.0 with 10 mmol·L^{-1} DTT, the corresponding n values of the four micelles increased to 0.52, 0.49, 0.51, and 0.50, respectively, all exceeding 0.45, which suggests a transition to a release behavior mainly controlled by diffusion and swelling. This shift occurred as all PDEAEMA blocks underwent protonation while the reductive cleavage of disulfide crosslinks removed covalent constraints on the polymer chains, leading to a higher degree of micellar swelling. Upon entering the second stage, the n values of all micelles under both conditions dropped again below 0.43, indicating that drug release reverted to being governed by the combined effects of diffusion and erosion. Throughout the entire process, the k values of the polymeric micelles in both stages increased with decreasing pH and increasing reductant concentration, reflecting an overall acceleration of the drug release rate. Moreover, the k values under pH 5.0/10 mmol·L^{-1} DTT were consistently and significantly higher than those at pH 7.4/0 mmol·L^{-1} DTT. For example, for the C-MIX micelle, the k values in the two stages at pH 5.0/10 mmol·L^{-1} DTT were 0.088 and 0.111, respectively, both higher than the corresponding values of 0.060 and 0.071 at pH 7.4/0 mmol·L^{-1} DTT, validating the effective enhancement of the overall release rate by

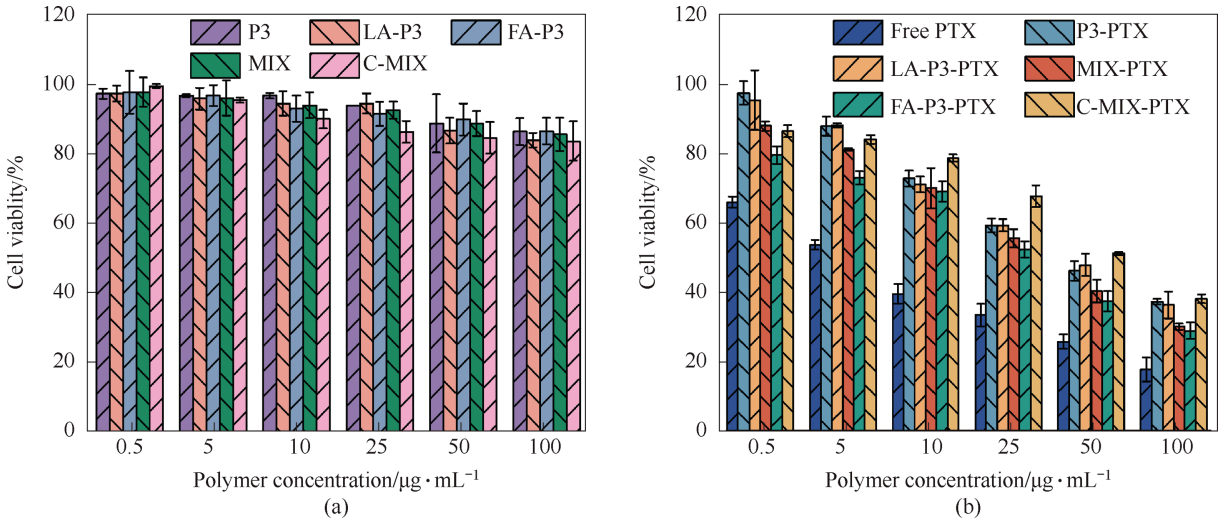


Fig. 7. Cell viability results of blank micelles (a) and PTX-loaded micelles (b).

Table 5
Comparison with previously reported folate- or disulfide-based micellar systems.

Polymer	Drug loading/%	Release rate/%	Cytotoxicity(IC_{50})/μg·ml^{-1}	Reference
HM-PMss/CTX	8.39	88 (120 h)	50.4	[31]
FA-PLL(SA)-PLA/DOX	5.82	40.7 (72 h)	5(DOX)	[32]
CCL/FA/DOX	9.5	96 (48 h)	29.00(DOX)	[33]
FHCSPBA-I	14.6	59.4 (170 h)	16.4	[34]
C-MIX-PTX	15.31	77.14 (120 h)	61.45	Our work

the pH/reduction dual-responsive behavior. Additionally, the non-crosslinked MIX system exhibited higher release rate constants under both simulated conditions, which is attributed to the absence of a crosslinked network, allowing the drug to diffuse out at the maximum possible rate. In contrast, C-MIX showed lower release rate constants than MIX, demonstrating that the successfully constructed disulfide crosslinked network effectively retarded the burst release and endowed the drug-loaded micelles with improved controlled-release characteristics.

Therefore, based on the comprehensive analysis of the release mechanisms and results, it can be concluded that the pH- and reduction-dependent C-MIX@PTX system could selectively respond to the tumor microenvironment, enabling on-demand control of drug release and thereby improving therapeutic efficacy.

3.4. Cytotoxicity assessment

The cytotoxicity of copolymer P3, LA-P3, FA-P3, MIX, mixed crosslinked blank micelles (C-MIX), free DOX, and PTX-loaded micelles (P3@PTX, LA-P3@PTX, FA-P3@PTX, MIX@PTX, C-MIX@PTX) against HepG2 cells was evaluated using the CCK-8 assay. As shown in Fig. 7(a), LA and FA modifications of copolymer P3 caused minimal changes in cytotoxicity toward HepG2 cells. Both MIX and C-MIX exhibited comparable cytotoxicity, with cell viability exceeding 80% after 48 h of incubation. These results confirmed that all synthesized polymers in this work possessed good biocompatibility and low cytotoxicity. Fig. 7(b) demonstrated that all PTX-loaded micelles prepared in this work exhibited inhibitory effects on HepG2 cells. Among them, FA-P3@PTX showed the lowest cell viability (28.9% at 100 $\mu g \cdot ml^{-1}$ after 48 h incubation), indicating stronger inhibition by FA-modified micelles. The crosslinked C-MIX@PTX exhibited slightly weaker inhibition, which was attributed to the decrosslinking step required during PTX release, and led to slower PTX release kinetics. The mixed micelles MIX@PTX displayed inhibition comparable to FA-P3@PTX, with significantly enhanced efficacy compared to P3@PTX. Combined with the *in vitro* PTX release profiles, it was predicted that C-MIX@PTX would achieve potent inhibition against HepG2 cells upon complete PTX release. Furthermore, the IC_{50} values for free PTX and the polymer-loaded drug micelles MIX-PTX and C-MIX@PTX were determined to be 6.31, 30.73 and 61.45 $\mu g \cdot ml^{-1}$, respectively. These results indicated that the polymeric material itself exhibited minimal cytotoxicity. Moreover, the PTX-loaded crosslinked micelles could effectively kill cancer cells while maintaining controlled drug release, demonstrating their potential as an excellent drug carrier material.

According to the comparative data presented in Table 5, the carrier developed in this study demonstrates superior performance in terms of drug loading capacity, prevention of burst release, controllability of release rate, and tunable cytotoxicity when compared to previously reported systems, indicating its promising potential for practical application.

4. Conclusions

In summary, three pH-responsive block copolymers P1, P2, and P3 with varying block ratios were synthesized *via* bromination, ROP, andATRP. The structures, molecular weights, and distributions of the copolymers were characterized using ^1H NMR, FT-IR, and GPC. Comprehensive comparisons of CMC and PTX loading performance among P1, P2, and P3, it was revealed that P3 exhibited optimal comprehensive PTX delivery performance for PTX. P3 was further modified through esterification to introduce LA and FA, yielding LA-P3 and FA-P3, which were successfully synthesized and characterized. MIX were prepared at a mass ratio of 1:1 (LA-P3:FA-P3), followed by self-crosslinking initiated by DTT to obtain C-MIX. The sizes results demonstrated that the TEM of PTX-loaded micelles (LA-P3@PTX, FA-P3@PTX, MIX@PTX, and C-MIX@PTX) prepared at a feeding ratio of 15 mg PTX/30 mg polymer were consistent with those determined by DLS: 135.8, 121.3, 144.9 and 134.7 nm, respectively. The C-MIX@PTX exhibited a DLC of 15.31% ± 1.79% and an EE of 38.42% ± 5.22%, which were comparable to those of the mixed non-crosslinked PTX-loaded micelles. Under neutral conditions, C-MIX@PTX micelles exhibited a cumulative PTX release of 16.8% at 120 h, while under tumor conditions, a fast and cumulative release of 77.1% at 120 h was obtained. After 48 h incubation, LA-P3@PTX, FA-P3@PTX, MIX@PTX, and C-MIX@PTX exhibited inhibitory effects on HepG2 cells, with FA-P3@PTX showing enhanced efficacy. Therefore, the pH/reduction dual-responsive crosslinked mixed micelles modified with FA and LA developed in this work demonstrate improved stability, targeting capability, and controlled-release capacity for PTX, suggesting potential for application in targeted drug delivery.

CRediT Authorship Contribution Statement

Minghong Feng: Writing – original draft, Validation, Investigation, Conceptualization. Teng He Validation, Conceptualization. Haiqian Zhao: Validation, Data curation. Tao Chen: Investigation, Formal analysis. Wenjing Lin: Writing – review & editing, Supervision, Project administration, Methodology, Funding acquisition, Conceptualization. Chufen Yang: Writing – review & editing, Supervision, Project administration, Funding acquisition.

Declaration of Competing Interest

The authors declare that they have no known competing financial interests or personal relationships that could have appeared to influence the work reported in this paper.

Acknowledgements

The authors gratefully acknowledge the financial support from the National Natural Science Foundation of China (21676058, 21808039), the Guangdong Basic and Applied Basic Research Foundation (2016A030313694, 2024A1515011182), the Guangzhou Basic and Applied Basic Research Foundation (2023A04J0064).

Supplementary Material

Supplementary data to this article can be found online at https://doi.org/10.1016/j.cjche.2026.01.013.

References

[1] S.K. Hari, A. Gauba, N. Shrivastava, R.M. Tripathi, S.K. Jain, A.K. Pandey, Polymeric micelles and cancer therapy: an ingenious multimodal tumor-targeted drug delivery system, *Drug Deliv. Transl. Res.* 13 (1) (2023) 135–163.
[2] Z. Li, J.H. Zou, X.Y. Chen, In response to precision medicine: current subcellular targeting strategies for cancer therapy, *Adv. Mater.* 35 (21) (2023) e2209529.
[3] F. Chen, L. Yin, T. He, T. Chen, H.B. Yue, C.F. Yang, Fabrication of dual pH/reduction-responsive P(CL-*co*-ACL)-based cross-linked polymeric micelles for PTX delivery, *Langmuir* 39 (46) (2023) 16358–16366.
[4] H.X. Wei, M.H. Liu, T.Y. Wang, M.H. Shih, J. Yu, Y.C. Yeh, Fabrication of pH- and ultrasound-responsive polymeric micelles: the effect of amphiphilic block copolymers with different hydrophilic/hydrophobic block ratios for self-assembly and controlled drug release, *Biomacromolecules* 26 (4) (2025) 2116–2130.
[5] A.Z. Juthi, M. Aquib, M.A. Farooq, S. Ghayas, F. Khalid, G.F. Boafo, D.P. Wande, D.H. Khan, T.Z. Bithi, R. Bavi, B. Wang, Theranostic applications of smart nanomedicines for tumor-targeted chemotherapy: a review, *Environ. Chem. Lett.* 18 (5) (2020) 1509–1527.

[6] Y.F. Cai, J.P. Qi, Y. Lu, H.S. He, W. Wu, The *in vivo* fate of polymeric micelles, *Adv. Drug Deliv. Rev.* 188 (2022) 114463.
[7] Z.Q. Zhang, X.X. Xu, J.W. Du, X. Chen, Y.E. Xue, J.Q. Zhang, X. Yang, X.Y. Chen, J. B. Xie, S.H. Ju, Redox-responsive polymer micelles co-encapsulating immune checkpoint inhibitors and chemotherapeutic agents for glioblastoma therapy, *Nat. Commun.* 15 (1) (2024) 1118.
[8] T. Ozbek, H. Demir, S. Dokuz, S. Tasdurmazli, U. Ozbey, M. Ozbil, M. Topuzogullari, I. Cinar, M. Karamese, S.A. Karamese, S. Acar, O.F. Bayrak, E. Cadirci, Phage-inspired targeting of antibiotic-loaded polymeric micelles for enhanced therapeutic efficacy against monomicrobial sepsis, *J. Contr. Release* 380 (2025) 773–786.
[9] D. Wan, S.F. Li, J.X. Zhang, G.L. Ma, J. Pan, Intelligent self-assembly prodrug micelles loading doxorubicin in response to tumor microenvironment for targeted tumors therapy, *Chin. J. Chem. Eng.* 39 (2021) 219–227.
[10] X.H. Pu, L.L. Zhao, J. Li, R.F. Song, Y.L. Wang, K.K. Yu, X.Q. Hou, P. Qiao, L.L. Zong, S. Chang, A polymeric micelle with an endosomal pH-sensitivity for intracellular delivery and enhanced antitumor efficacy of hydroxycamptothecin, *Acta Biomater.* 88 (2019) 357–369.
[11] K.J. Luo, W.X. Guo, Y.T. Yu, S.M. Xu, M. Zhou, K.Q. Xiang, K. Niu, X.Q. Zhu, G.Y. Zhu, Z. An, Q.S. Yu, Z.H. Gan, Reduction-sensitive platinum (IV)-prodrug nano-sensitizer with an ultra-high drug loading for efficient chemo-radiotherapy of Pt-resistant cervical cancer *in vivo*, *J. Contr. Release* 326 (2020) 25–37.
[12] M.Q. Wang, J.R. Long, S.M. Zhang, F.J. Liu, X.L. Zhang, X.S. Zhang, L. Sun, L.W. Ma, C.Y. Yu, H. Wei, Folate-targeted anticancer drug delivery *via* a combination strategy of a micelle complex and reducible conjugation, *ACS Biomater. Sci. Eng.* 6 (3) (2020) 1565–1572.
[13] Y. Lu, E.S. Zhang, J.H. Yang, Z.Q. Cao, Strategies to improve micelle stability for drug delivery, *Nano Res.* 11 (10) (2018) 4985–4998.
[14] L. Zhang, R.B. Guo, M.H. Chen, M. Liu, Y. Liu, Y. Yu, J. Zang, L. Kong, X.T. Li, Inhibition of ovarian cancer growth, metastasis and reverse the tumor microenvironment by dual drug-loaded polymer micelle targeting tumor microenvironment, *Int. J. Nanomed.* 20 (2025) 2969–2990.
[15] Y.G. Wu, S.B. Chen, J.T. Zhu, Hydrogen-bond-driven core-crosslinked supramolecular micelles with pH/thermal/glutathione-responsive drug release toward enhanced cancer therapy, *Chem. Mater.* 35 (18) (2023) 7655–7670.
[16] J. Kaur, M. Gulati, N.K. Jha, J. Disouza, V. Patravale, K. Dua, S.K. Singh, Recent advances in developing polymeric micelles for treating cancer: breakthroughs and bottlenecks in their clinical translation, *Drug Discov. Today* 27 (5) (2022) 1495–1512.
[17] A.B. Ebrahim Attia, Z.Y. Ong, J.L. Hedrick, P.P. Lee, P.L.R. Ee, P.T. Hammond, Y. Y. Yang, Mixed micelles self-assembled from block copolymers for drug delivery, *Curr. Opin. Colloid Interface Sci.* 16 (3) (2011) 182–194.
[18] M. Cagel, F.C. Tesan, E. Bernabeu, M.J. Salgueiro, M.B. Zubillaga, M.A. Moretton, D.A. Chiappetta, Polymeric mixed micelles as nanomedicines: achievements and perspectives, *Eur. J. Pharm. Biopharm.* 113 (2017) 211–228.
[19] A.M. Butt, M.C.I.M. Amin, H. Katas, N.A. Abdul Murad, R. Jamal, P. Kesharwani, Doxorubicin and siRNA codelivery *via* chitosan-coated pH-responsive mixed micellar polyplexes for enhanced cancer therapy in multidrug-resistant tumors, *Mol. Pharm.* 13 (12) (2016) 4179–4190.
[20] Z.L. Cao, X.L. Zuo, X.C. Liu, G.X. Xu, K.T. Yong, Recent progress in stimuli-responsive polymeric micelles for targeted delivery of functional nanoparticles, *Adv. Colloid Interface Sci.* 330 (2024) 103206.
[21] C.F. Yang, W.Y. Liu, J.Y. Xiao, C. Yuan, Y.X. Chen, J.W. Guo, H.B. Yue, D.Y. Zhu, W.J. Lin, S.Q. Tang, X.Y. Dong, pH-sensitive mixed micelles assembled from PDEAEMA-PPEGMA and PCL-PPEGMA for doxorubicin delivery: experimental and DPD simulations study, *Pharmaceutics* 12 (2) (2020) 170.
[22] C.F. Yang, D.L. Wang, W.Y. Liu, Z.X. Yang, T. He, F. Chen, W.J. Lin, Folate modified dual pH/reduction-responsive mixed micelles assembled using FA-PEG-PDEAEMA and PEG-SS-PCL for doxorubicin delivery, *Phys. Chem. Chem. Phys.* 25 (17) (2023) 12458–12468.
[23] W.Q. Yang, P.W. Chen, E. Boonstra, T. Hong, H. Cabral, Polymeric micelles with pH-responsive cross-linked core enhance *in vivo* mRNA delivery, *Pharmaceutics* 14 (6) (2022) 1205.
[24] J.J. Sun, Z. Wang, A.M. Cao, R.L. Sheng, Synthesis of crosslinkable diblock terpolymers PDPA-b-P(NMS-co-OEG) and preparation of shell-crosslinked pH/redox-dual responsive micelles as smart nanomaterials, *RSC Adv.* 9 (59) (2019) 34535–34546.
[25] Y.T. Zheng, Y. Oz, Y.M. Gu, N. Ahamad, K. Shariati, J. Chevalier, D. Kapur, N. Annabi, Rational design of polymeric micelles for targeted therapeutic delivery, *Nano Today* 55 (2024) 102147.
[26] D. Xiong, L.Y. Wen, S.Y. Peng, J.C. Xu, L.J. Zhang, Reversible cross-linked mixed micelles for pH triggered swelling and redox triggered degradation for enhanced and controlled drug release, *Pharmaceutics* 12 (3) (2020) 258.
[27] G.Z. Kuang, Q.F. Zhang, S.S. He, Y.J. Wu, Y.B. Huang, Reduction-responsive disulfide linkage core-cross-linked polymeric micelles for site-specific drug delivery, *Polym. Chem.* 11 (44) (2020) 7078–7086.
[28] C.F. Yang, J.Y. Xiao, W.F. Xiao, W.J. Lin, J.R. Chen, Q. Chen, L.J. Zhang, C.Y. Zhang, J.W. Guo, Fabrication of PDEAEMA-based pH-responsive mixed micelles for application in controlled doxorubicin release, *RSC Adv.* 7 (44) (2017) 27564–27573.
[29] L. Cai, X.J. Qin, Z.H. Xu, Y.Y. Song, H.J. Jiang, Y. Wu, H.J. Ruan, J. Chen, Comparison of cytotoxicity evaluation of anticancer drugs between real-time cell analysis and CCK-8 method, *ACS Omega* 4 (7) (2019) 12036–12042.
[30] P.L. Ritger, N.A. Peppas, A simple equation for description of solute release I. Fickian and non-fickian release from non-swellable devices in the form of slabs, spheres, cylinders or discs, *J. Contr. Release* 5 (1) (1987) 23–36.
[31] X.X. Han, F.R. Gong, L.L. Chi, C.C. Feng, J. Sun, Y.Y. Chen, J.W. Liu, Y.L. Shen, Cancer-targeted and glutathione-responsive micellar carriers for controlled delivery of cabazitaxel, *Nanotechnology* 30 (5) (2019) 055601.
[32] J. Guan, Z.Q. Zhou, M.H. Chen, H.Y. Li, D.N. Tong, J. Yang, J. Yao, Z.Y. Zhang, Folate-conjugated and pH-responsive polymeric micelles for target-cell-specific anticancer drug delivery, *Acta Biomater.* 60 (2017) 244–255.
[33] X.Q. Yi, D. Zhao, Q. Zhang, J.Q. Xu, G.D. Yuan, R.X. Zhuo, F. Li, Preparation of multilocation reduction-sensitive core crosslinked folate-PEG-coated micelles for rapid release of doxorubicin and tariquidar to overcome drug resistance, *Nanotechnology* 28 (8) (2017) 085603.
[34] L.L. Zhao, Y.J. Zhang, J. Shao, H.Z. Liang, H.N. Na, J. Zhu, Folate-conjugated dually responsive micelles for targeted anticancer drug delivery, *RSC Adv.* 6 (42) (2016) 35658–35667.